Cold State-Selected Molecular Collisions and Reactions

Benjamin K. Stuhl,[1] Matthew T. Hummon,[2] and Jun Ye[2]

[1]Joint Quantum Institute, National Institute of Standards and Technology and University of Maryland, Gaithersburg, Maryland 20899

[2]JILA, National Institute of Standards and Technology and University of Colorado, Boulder, Colorado 80309; email: ye@jila.colorado.edu

Keywords

Abstract

Over the past decade, and particularly the past five years, a quiet revolution has been building at the border between atomic physics and experimental quantum chemistry. The rapid development of techniques for producing cold and even ultracold molecules without a perturbing rare-gas cluster shell is now enabling the study of chemical reactions and scattering at the quantum scattering limit with only a few partial waves contributing to the incident channel. Moreover, the ability to perform these experiments with nonthermal distributions comprising one or a few specific states enables the observation and even full control of state-to-state collision rates in this computation-friendly regime: This is perhaps the most elementary study possible of scattering and reaction dynamics.

1. INTRODUCTION

It is a truism in atomic physics that "colder is cleaner." At ultralow temperatures, all two-body scattering processes converge to the limit of a single quantum mechanical partial wave, wherein the entire dynamics of the system can be determined from the scattering length a (1, 2). Reactive molecular scattering is of course more than a two-body process, but low temperatures continue to greatly simplify the problem (3–5): Subkelvin temperatures freeze out both rotational and vibrational dynamics and reduce the number of contributing partial waves to a low-enough value that one can perform true quantum scattering calculations. Low temperatures also enable the detailed study of phenomena such as hyperfine-mediated reactions (6), whose energy scales are entirely unresolvable at room temperature. Moreover, at these low temperatures, both scattering and reaction dynamics are often dominated by relatively simple, long-range interactions that sidestep a great deal of short-range chemical complexity to produce universal behaviors (7–10). This article seeks to provide an introduction to several leading techniques for performing cold collision experiments and discusses some recent highlights of the field. By necessity, this is not intended to be a more general or exhaustive review of the entire field of cold molecules: Readers in search of such are suggested to consider References 11–16, with particular attention to the most recent ones as a great deal of progress has been made in the past five years.

2. CREATING COLD MOLECULES

Efforts to study subkelvin chemistry are not new: Techniques such as rare-gas cluster spectroscopy (17–19) have been used for more than 25 years. However, this technique involves embedding the species of interest within a shell of loosely bound rare-gas atoms. This shell hinders the motion of the molecules within it and creates systematic shifts in both spectroscopy and reaction dynamics relative to true vacuum binary collisions. Superfluid helium nanodroplets (20–23) provide a much closer approximation to a vacuous environment, although the droplet's presence remains a constant. Recent improvements in pulsed-valve technology (24–26) have enabled the production of cryogenic supersonic beams, which in a crossed-beam geometry allow access to single-kelvin energy scales (27). Other techniques, such as noncryogenic molecular beams (28) and their more recent refinements, including the CRESU (Cinétique de Réaction en Ecoulement Supersonique Uniforme) uniform Laval jet (11, 29–32), cannot reach such low collision energies. On a different path, the relative ease of trapping charged species—and the rapid thermalization rates they can achieve (33)—has enabled impressive results in ion-molecule reaction studies (34, 35). Kinematic techniques that use rotationally inelastic collisions with a counterpropagating atomic beam are able to produce translationally cold but rotationally excited molecular samples (36–38). For all these techniques, the state distribution of the collision partners is thermal: Such beams can only be considered state selective if the temperature is low enough to freeze out all relevant excitations. (This thermal limit can be side stepped by state-filtering techniques, which are discussed in the next two sections.) For hydrides, temperatures of the order of 10 K suffice to freeze out rotations, but even the prototypical light molecule CO has a rotational constant of only 1.93 cm^{-1}. At the 2.2-K lambda point of ^{4}He, almost 20% of CO molecules remain rotationally excited, and the heavier the molecule is, the higher the excited fraction (39). With regard to scattering, still lower kinetic temperatures are required to access the few-partial-wave regime, as the energy scale for the multiparticle centrifugal barrier associated with a nonzero angular momentum partial wave is always much smaller than the molecule's rotational constant.

Another technique—which yields extremely low temperatures and full quantum state control—deserves a brief mention, although it is out of the scope of this article. The method of Feshbach

association and stimulated Raman adiabatic passage (STIRAP) state transfer (40, 41) has been used with great success to produce the only submicrokelvin samples of heteronuclear molecules. By separately cooling the starting ^{87}Rb and ^{40}K atoms and then coherently combining the two atoms into a bound, ground-state molecule, Ni et al. (41) were able to produce molecules at a temperature and density near Fermi degeneracy. In this ultracold regime, virtually all the molecules occupy a single internal ground state, so chemistry is dominated by the quantum statistics and spatial extent of the molecular wave function in a way that is quite alien to an intuition developed near room temperature. Specifically, they were able to observe Fermi-repulsion-controlled chemistry, in which population-averaged rates for the recombination reaction

$$2KRb \rightarrow Rb_2 + K_2 \qquad (1)$$

were set by the degree of hyperfine polarization in the sample (6). The ultralow temperature also permits the KRb molecules to be confined in optical lattices (42), allowing the control of chemistry by directly varying the molecular scattering rate. The association-plus-STIRAP technique, however, is currently restricted to only ^{40}K^{87}Rb, although efforts are in progress to extend it to other bialkali and alkali-metal/alkali-earth systems, such as LiCs (9, 43–45), RbCs (46), RbSr (47, 48), LiYb (49, 50), and RbYb (51).

2.1. State-Selective Guiding

Production of a state-purified sample usually follows one of two paths: Either the desired state is filtered out of a larger, mixed-state sample, or the desired state is selectively populated through thermal equilibration (for the specific case of the ground state) or some sort of nonthermal pumping (e.g., optical pumping or resonant photodissociation). Filter techniques commonly involve selective guiding or focusing of molecules in one state, whereas all others are defocused and blocked by a mechanical barrier or simply escape the guide and are pumped away.

Molecules respond to both AC and DC electromagnetic field gradients and usually with at least some state specificity. Far-off-resonant AC fields are in general the least state selective, or a more careful choice of the AC frequency relative to the polarizability spectra of the relevant states can produce truly state-insensitive forces, as in optical magic wavelength traps (52); near-resonant fields act much more strongly on those states involved in said resonance. Static fields couple to the permanent electric or magnetic dipole moments of the molecule, and these moments are state dependent owing to parity, rotational averaging of the orientation of the moments, and vibrational averaging of the magnitude of the electric dipole moment. Most commonly, because static fields can possess only free-space minima and not maxima, molecules are guided in an electric or magnetic weak-field-seeking state, for example, in hexapole guides (53–55).

These static-field guides are almost the simplest system imaginable for controlling the motion of selected states. As illustrated in **Figure 1**, static guides simply create a quasi-tubular field distribution with a transverse minimum of the field at the center. In their weak-field-seeking states, molecules are guided down this tube, with a confinement strength proportional to the state's Stark or Zeeman shift. Different field geometries produce varying transverse curvatures of the guiding potential; in particular, a dipolar particle in a hexapole field experiences an approximately harmonic confinement. The harmonic case is special because the oscillation frequency within a harmonic oscillator is independent of the oscillation amplitude. This means that a distribution of molecules transversely diverging from a point source is refocused to a unique point by a hexapole, if the longitudinal velocities are the same. Because the depth of the confining potential—and therefore its curvature—is state dependent, the focal length of a hexapole is also state dependent.
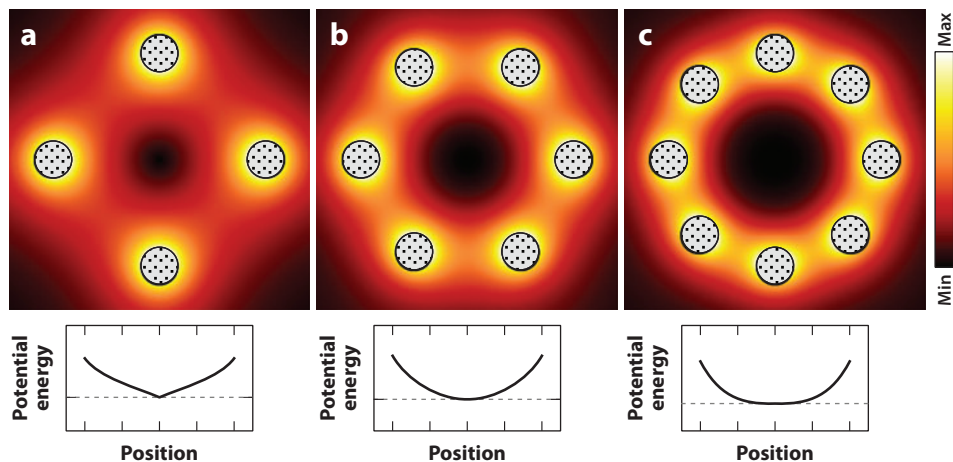
Figure 1

Trap potentials for realistic linear electrostatic (*a*) quadrupole, (*b*) hexapole, and (*c*) octopole guides, as calculated by finite-element methods. The color denotes the potential energy possessed by a dipolar particle at that position. The hashed regions indicate the cross-sectional area of the electrodes. (*Lower panels*) Cuts along the horizontal symmetry line of each guide. Horizontal scales are matched between the images and the graphs.

All this has been known since the 1950s in the case of electrostatic guides and can really be thought of as a simple extension of the Stern-Gerlach effect. What is much more recent is the use of a guide as not only a state filter, but also a velocity filter. A simple curved guide acts as a low-pass velocity filter because it has a finite depth to its confining potential: Molecules whose kinetic energy exceeds that depth are unguided and therefore escape. This effect has been used to filter many different cold molecules out of thermal distributions, including the original demonstration by Rangwala et al. (56) with H_2CO and ND_3 and more recent experiments involving water and its isotopologs (55, 57). Switching the guide adds control of the minimum guided velocity, as well as the maximum, and so enables the production of narrow, velocity-selected pulses (58).

2.2. Stark and Zeeman Deceleration

The production of denser cold beams than are available from a thermal distribution requires a more active technique than simple guiding. Stark (59–62) or Zeeman (63–66) deceleration uses pulsed electric or magnetic fields, respectively, to slow the cold, but fast packet produced by a supersonic expansion (28). These packets commonly have internal rotational temperatures of a few kelvin and comoving translational temperatures of the same order but have a mean center-of-mass velocity of hundreds of meters per second. Vibrational excitations are poorly quenched by supersonic expansions, so vibrational degrees of freedom can be substantially out of equilibrium with the others (67, 68). Decelerators remove the center-of-mass velocity and can bring the coldest fraction of the packet to rest in the laboratory frame so that the molecules can be confined in a trap (69–72).

Both Stark and Zeeman decelerators (the latter are also sometimes called coilguns to distinguish them from the Zeeman slowers of atomic physics, which are fundamentally laser cooling devices) operate on the same general principle (62, 73, 74). The atom or molecule of choice is in a weak-field-seeking state, so as it enters a high-field region, it effectively rides up a potential

hill and is slowed. Before the particle crests this hill, the field is rapidly switched off so that the potential energy possessed by the particle is permanently removed. This process does not provide any cooling to a particle distribution, as the slowing force is independent of the particle's velocity, but it does provide spatial confinement and the removal of mean velocity. Moreover, because the guidance and slowing are both state dependent, decelerators also provide very high selectivity on those states whose quantum numbers affect the electric or magnetic dipole moment of the molecule. The notable exception is the vibrational quantum number v, as the response of the molecule to external fields varies only weakly with increasing v near $v = 0$. Currently under development is a more advanced form of decelerator, in which the particles are held in an effective traveling potential well, which adiabatically slows down and drags the packet to a stop (75, 76).

2.3. Buffer-Gas Cooling

Another common technique for producing cold, state-selected molecules is buffer-gas cooling (77, 78). This method is quite different from the two discussed above in that it explicitly uses a cryogenic system to reduce the molecules' temperature, rather than any form of nonthermal filtering. Buffer-gas cooling, as its name implies, thermalizes the species of interest through collisions with a helium buffer gas within a cryogenic cell. An aperture in the cell allows the escape of helium and, with it, an entrained beam of the cooled target species. Molecules can be introduced to the cell directly as gases (79, 80), through laser ablation of an in situ target (81), or from an external beam source (77). ^{4}He buffer gas permits beam temperatures as low as 1 K, limited by the vapor pressure of ^{4}He; ^{3}He permits temperatures as low as 240 mK (82).

The dynamics of the buffer-gas beam formation process varies widely with the density of the helium gas (78). At very low densities, the beam is effusive, and the target molecules exit the cell with a thermal velocity distribution matching the cell temperature; however, the beam intensity is very low, as most target molecules freeze to the cell walls rather than escape through the aperture. At high helium densities, a supersonic expansion can form, causing the target molecules to rotationally cool below the cell temperature and be efficiently extracted from the cell through entrainment in the helium flow, but they exit with a mean velocity of the order of 150 m/s for a 4-K cell temperature (78). At intermediate densities, there is the so-called hydrodynamic regime, in which the beam velocity is lower and approximately equal to the helium thermal velocity but the cell extraction efficiency remains good (53). A major topic of ongoing research in the field is the reduction of the target molecule velocity to the effusive regime while maintaining good extraction efficiencies; current efforts involving a secondary, lower-pressure cell are extremely promising, although more complex than a single-cell design (78, 83).

Once the molecular beam has exited its source cell, it is often necessary to separate it from the helium carrier gas. This is easily accomplished using one of the state-selective guides discussed in Section 2.1. If the guide is given an appreciable bend, the state-selected fraction is separated from the carrier gas, which can then be pumped away (53, 80). At the most extreme bending angle, a full 90° bend provides very efficient differential pumping in addition to strong velocity filtering (80, 84, 85). The guide also provides confinement of the beam for efficient long-distance transport (e.g., to allow the beam to exit the cryogenic region into a room-temperature experimental section).

Buffer-gas experiments can also be conducted without the requirement of beam formation. Superconducting magnets can create the multi-Tesla fields needed to trap paramagnetic atoms or molecules at kelvin-scale temperatures, so the trap can be continually loaded simply through thermalization with the helium buffer gas. The buffer gas can then be removed, allowing long trap lifetimes (81, 82, 86, 87).

LASER COOLING MOLECULES

Laser cooling has been the workhorse technique of atomic physics for the past 35 years (138, 139). Because many atoms have only one or two ground states, they can resonantly scatter millions of photons without being bleached by optical pumping into a metastable level. With the appropriate choice of laser frequency, the recoil of the photons can cool the atom. Molecules, however, effectively possess a huge number of ground states: The radiative decay of rovibrational excitations is extremely slow. Additional lasers can optically pump molecules back out of these metastable levels, but the number of lasers needed was long considered to be completely impractical (140).

This has changed within the past five years. Although molecules generally remain impractical to cool with lasers, there is a small but substantial class of molecules that are amenable to the technique. Molecules that have extremely diagonal Franck-Condon matrices and also support certain rotational selection rules can cycle thousands or tens of thousands of photons with as few as three distinct lasers. The challenge is that, whereas normal atomic laser cooling tends to be self-spin-polarizing, the selection rule needed to prevent rotational state diffusion means that molecular laser cooling is depolarizing and tends to drive the molecules into optically passive dark states. Our group originally pointed out the utility of the selection rules and proposed a solution to the dark-state issue, using TiO as the exemplar molecule (141). Laser cooling has now been experimentally demonstrated in SrF (142–144), YO (145), and CaF (146). Furthermore, it is now proven that molecules can be confined in magneto-optical potentials (145), which will be the ideal starting point for further cooling and confinement in optical potentials. The family of laser coolable molecules contains species that are too massive to efficiently Stark or Zeeman decelerate, so entirely new areas of collision studies will shortly be available.

2.4. Evaporative Cooling

All three of the above techniques suffer from a rapid loss of cooling power in the cold regime (13). Temperatures of a few tens of millikelvin are routinely achievable from Stark deceleration and a few hundred from buffer-gas cooling. However, it has been a long-standing challenge to find a method to cool from those lukewarm temperatures, at the upper limits of achievable trap depths, down to the tens-of-microkelvin regime needed for optical trapping or the submicrokelvin temperatures needed to produce quantum-degenerate gases—that is, cooling and compression to produce a factor of 10^{12} increase in phase-space density (13). One technique that has burst into prominence over the past several years is the application of atomic laser cooling methods to selected molecules (see the sidebar, Laser Cooling Molecules). Another possibility, only recently demonstrated (88), is evaporative cooling.

The preferred technique for cooling atomic gases to quantum degeneracy has always been evaporative cooling—that is, the selective removal of the highest-energy particles from a thermal distribution, while re-equilibration proceeds via collisions sufficiently rapidly that the sample remains approximately thermal and the high-energy tail is continuously repopulated (2, 89, 90). Atoms, however, are simple: Two-body atomic collisions can only cause trap loss due to spin depolarization. Not only are spin-changing collisions strongly suppressed in most atoms (1), but optical traps, for instance, are state insensitive. Three-body collisions can of course cause recombination into dimers and thus the loss of atoms, but for many species, the three-body rate constants are small (1, 90). Polar molecules, by contrast, collide on highly anisotropic potential surfaces, so it was long believed that inelastic state-changing collisions would be too common to permit adequate thermalization and efficient evaporation (13, 91–96).

Recent theoretical studies began to question this belief (97–100). Proposals to suppress these inelastic collisions to allow for efficient evaporative cooling include dressing the molecules with
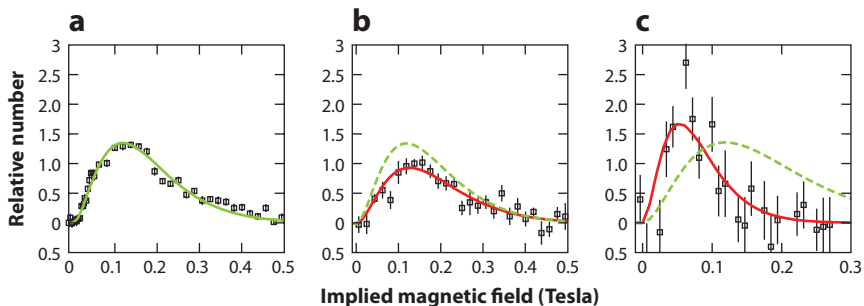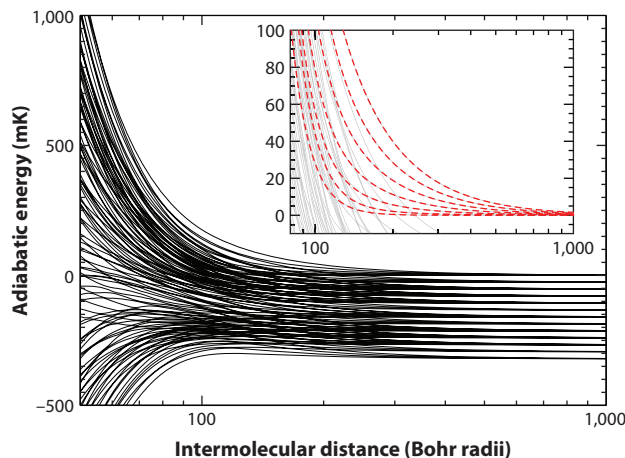
Figure 2

Microwave Zeeman spectra of magnetically trapped OH molecules, demonstrating three different temperatures: (*a*) the initial distribution at 55 mK, (*b*) forced antievaporation (selective removal of the coldest molecules) to 59 mK, and (*c*) evaporative cooling to 25 mK. The solid lines are fits to a Boltzmann distribution. The green dashed lines reproduce the form of the initial distribution for comparison. Note the change of horizontal scale in panel *c*. Figure modified from Reference 88.

microwave fields (101) or confining molecules to a two-dimensional (2D) geometry (102). In both these cases, a long-range repulsive interaction is deliberately engineered to prevent molecules from experiencing short-range interactions that lead to inelastic loss. In the work of de Miranda et al. (102), the 2D geometry led to suppression of inelastic chemical loss by two orders of magnitude, but momentum exchange in 2D elastic collisions was not efficient enough for evaporative cooling to reach below the Fermi temperature.

Most recently, our group observed evidence for evaporative cooling in magnetically trapped OH molecules (88). By using an electric-dipole microwave transition to selectively remove molecules found at potential energies much larger than $\frac{3}{2}k_B T$, we were able to cool the sample from 55 mK to 25 mK while the number of molecules was only reduced by a factor of 2, as illustrated in **Figure 2**. The open-shell $^2\Pi_{3/2}$ ground state of OH gives each rotational level a closely spaced parity doublet. The molecules are magnetically trapped in the weak-field-seeking Zeeman sublevel of the upper parity state, loaded from a Stark decelerator (72, 103). In that state, the intermolecular van der Waals interaction becomes positive and creates a large, repulsive scattering barrier at separations of the order of 100 Bohr radii, which suppresses shorter-range inelastic interactions (88, 104). This large, repulsive scattering barrier should be a generic feature for molecules whose parity doublet energy spacing is small compared to the rotational energy level spacing of the molecule. Moreover, inelastic processes in paramagnetic radicals are believed to be generically suppressed by the large magnetic fields present in the quadrupole trap (97). **Figure 3** shows the per-partial-wave adiabatic energies for magnetically trappable OH molecules, demonstrating the repulsive barrier.

3. COLD COLLISION STUDIES

Over the past decade, the rapid development of the techniques described above has allowed them to progress from research projects in their own right to tools that can be applied to perform experiments in pursuit of chemical or physical knowledge. In many ways, cold molecule techniques can now be applied similarly to a crossed-molecular-beam instrument or a surface-scattering instrument—except that the collisions have few-kelvin or even few-millikelvin kinetic energies; in most cases, the samples can be prepared in a single quantum state; and unlike surface-scattering experiments, the interactions can be reliably treated as being in the single-scatter limit.
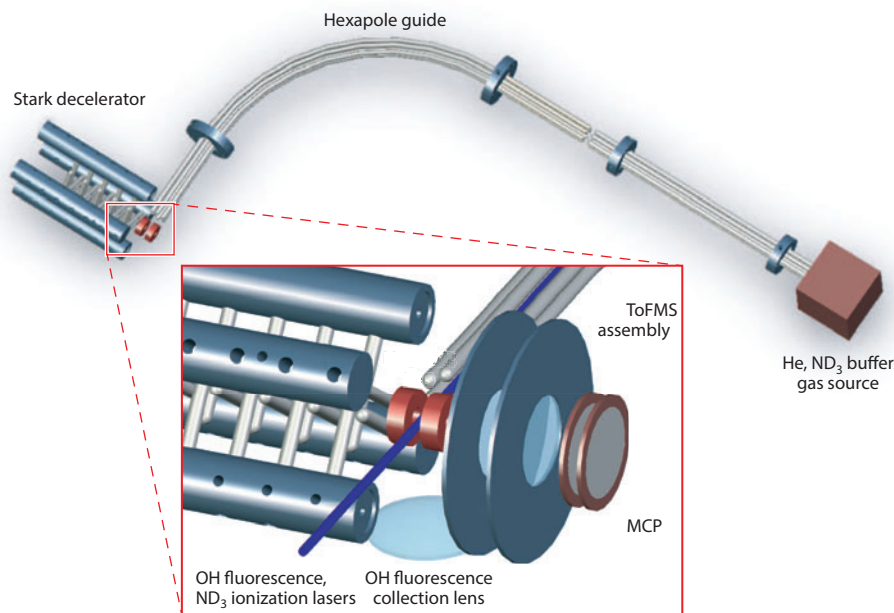
Figure 3

Adiabatic energies of $\ell = 0, 2, 4$, and 6 partial waves for two colliding OH molecules in their
$|^2\Pi_{3/2}, v = 0, J = \frac{3}{2}\rangle$ ground state, demonstrating the long-range barrier that protects against inelastic
losses during evaporation. (*Inset*) An expanded view of the uppermost long-range adiabat in the region of
100–1,000 Bohr radii. Magnetically trapped molecules collide with the partial waves of the uppermost
long-range adiabat, denoted by the dashed red lines in the inset. Figure modified from Reference 88 by
courtesy of G. Quéméner.

3.1. Trapped-Sample Experiments

Almost as soon as the first molecule traps were demonstrated, there was an immediate desire to
demonstrate their utility for collision experiments. The very first measurements made with trapped
molecules were mostly warm, such as van de Meerakker et al.'s (67) time-domain measurement
of the OH $v' = 1$ state radiative lifetime in an electrostatic trap loaded from a Stark decelerator
and Sawyer et al.'s (70) measurement of the OH-N_2 total scattering cross section at 295 K in a
magnetic trap also loaded from a Stark decelerator. Yet the intrinsically cold surroundings of a
buffer-gas-loaded trap made it easy for Weinstein et al. (81) to set limits on the CaH-He cross
sections at 300 mK.

This early divide between cryogenic and room-temperature traps continues to be substantially
reflected in the more recent literature. Sawyer et al. (72) proceeded stepwise to lower collision
energies, first by measuring OH-He and OH-D_2 cross sections from 300 K down to 77 K using
a liquid-nitrogen-cooled supersonic beam of He or D_2 to eject trapped OH molecules. The
impinging beam densities were calibrated using a capacitive microphone and a fast ionization
gauge; the total cross section was then fixed by comparing beam-trap collision rates and trap loss
rates when the chamber was filled to a known density of helium gas calibrated by a quadrupole mass
spectrometer residual gas analyzer. From 77 K, Sawyer et al. (80) proceeded down to 4 K, using
a buffer-gas system to produce a 100-m/s beam of ND_3 molecules, which were state and velocity
filtered by a 90° bent hexapole guide and then aimed through the trapped OH cloud (**Figure 4**).
The ND_3 beam density was determined by resonance-enhanced multiphoton ionization, which
was then cross-calibrated to a quadrupole mass spectrometer residual gas analyzer by backfilling the
vacuum chamber with 295-K ND_3. The broad rotational distribution of 295-K ND_3 compared to
the state-selected beam required substantial spectral modeling to determine the relative ionization
efficiencies of the two populations, which constituted the dominant systematic uncertainty in the
absolute cross-sectional values. Additionally, the authors observed evidence for dipole-mediated

Figure 4

Machine drawing of a cold collision experiment combining hexapole guiding, Stark deceleration, magnetic trapping, and buffer-gas cooling to measure the OH-ND$_3$ collision cross section at a temperature of 5 K. Figure reproduced from Reference 80. Abbreviations: MCP, microchannel plate; ToFMS: time-of-flight mass spectrometer.

scattering between OH and ND$_3$, with the cross section changing by a factor of 1.4 ± 0.3 between zero-field scattering conditions and scattering under an applied electric field sufficiently large to polarize both OH and ND$_3$.

There is an unfortunate complication to the interpretation of these beam-trap or even trap-background-gas collision experiments, in that the trap's own confining potential defines a minimum energy transfer required for an elastic collision to eject a molecule from the trap (105). This means that even at fairly high mean collision energies relative to the trap depth, the experiment's sensitivity to the forward-scattering part of the differential cross section is strongly suppressed. The observed trap loss cross section is therefore the sum of the inelastic cross section (assuming that all internal state changes cause trap loss) and some unknown, although theoretically calculable, fraction of the elastic cross section. When one accurately accounts for this effect, however, good agreement between experiment and scattering calculations is possible (105, 106).

Parazzoli et al. (96) took a different path to performing cold molecular scattering experiments and successfully colocated an electrostatically trapped sample of ND$_3$ loaded from a Stark decelerator with a rubidium magneto-optical trap. They put an upper bound on elastic and inelastic cross sections at a temperature of ∼100 mK, using magneto-optical trap fluorescence to determine the rubidium density. They also observed, and theoretically justified, electric-field effects resulting from the anisotropy of the Rb-ND$_3$ potential surface.

Buffer-gas systems have meanwhile continued to probe helium-scattering cross sections in a variety of molecules. Examples include Maussang et al.'s (107) measurement of Zeeman relaxation rates in CaF-He collisions at temperatures as low as 2 K, Campbell et al.'s (86) study of NH-He Zeeman relaxation at 2 K, and Lu & Weinstein's (108) study of TiO-He at 5 K. Successful

cotrapping of NH and atomic nitrogen allowed Hummon et al. (109) to measure elastic and inelastic cross sections for the fully spin-polarized NH-N system at ∼600 mK. Even without actually trapping either reactant, Singh et al. (110, 111) recently were able to measure the reaction rate of Li + CaH → LiH + Ca over the range 1–7 K owing to the long diffusion times intrinsic to large buffer-gas cells. Absolute calibration in these experiments is greatly simplified by the closed-cell geometry, which allows a simple pressure measurement to give a direct measurement of the mean helium density.

The recent recognition that the OH molecules in our Stark-decelerator-loaded magnetic trap are collisionally dense (88) has also allowed the study of OH-OH collision properties at 45 mK. Although it has proven extremely difficult to accurately determine the number and density distribution of trapped OH molecules, we were able to measure relative two-body loss rates as a function of electric field over a two-decade range from 100 to 10^4 V/cm. We observed a strong dependence of the loss rate on the field strength as the molecule was polarized (112).

3.2. Crossed- and Merged-Beam Techniques

Although gas-phase beam-on-target experiments are rare in the chemical literature, crossed-molecular-beam experiments are common. The replacement of the supersonic or effusive beam source with an equivalent slow beam source allows immediate reductions in the scattering energy scale. This has been elegantly demonstrated by Gilijamse et al. (113), who determined selected velocity-dependent, state-to-state inelastic cross sections for OH scattered by Xe atoms over an energy range of 50–400 cm^{-1} using a Stark-decelerated OH beam crossed at 90° by a supersonic Xe beam. Similar work has been extended to the rest of the stable rare gases in collision with OH (114–116), demonstrating, in general, excellent agreement between experiment and the detailed theoretical calculations available in these simple systems. Kirste et al. (114) also studied state-to-state inelastic scattering in the OH-D_2 system and observed good agreement with ab initio calculations over an energy range of 100–500 cm^{-1}. Collisions involving two heteronuclear molecules remain much harder to calculate, and the authors reported only fair agreement between theory and experiment in their most recent study of OH-NO scattering (117). All these experiments benefited greatly from the high energy resolution available with the Stark decelerator; similar experiments involving magnetic nonpolar species (e.g., O_2) are possible using the Zeeman decelerator (65, 66, 118).

Chefdeville et al. (27) took a more direct route to studying the rotational excitation of CO molecules in CO-H_2 collisions. By cooling a pair of fast pulsed valves (25) to cryogenic temperatures and crossing the resulting beams at a 12.5° angle, they were able to achieve rotational temperatures of the order of 1 K, yielding >95% and >99% rotational ground-state purity for *para*-H_2 and CO, respectively. This permitted a very clean measurement of the relative CO rotational excitation cross section over a 3–23-cm^{-1} collision energy span, with several observable—and calculable—resonance features in the spectrum.

Henson et al. (121) recently demonstrated a very different path to ultrahigh energy resolution in a study of orbital resonances in Penning ionization. It is a trivial matter of kinematics that the free flight of a gas packet through a vacuum establishes a correlation between position and velocity: Faster particles fly out in front, while slower particles lag to the back. For flights substantially longer than the packet's initial duration (set by the pulsed valve speed), it is therefore possible to spatially address a very narrow velocity class—one much narrower than the thermal width of the packet. By using a cryogenic supersonic expansion as the source, Henson et al. achieved energy resolutions as narrow as 0.8 mK, with a mean energy of 8.7 mK. This enabled them to observe orbital resonances in He*-H_2 and He*-Ar Penning ionization (**Figure 5**).
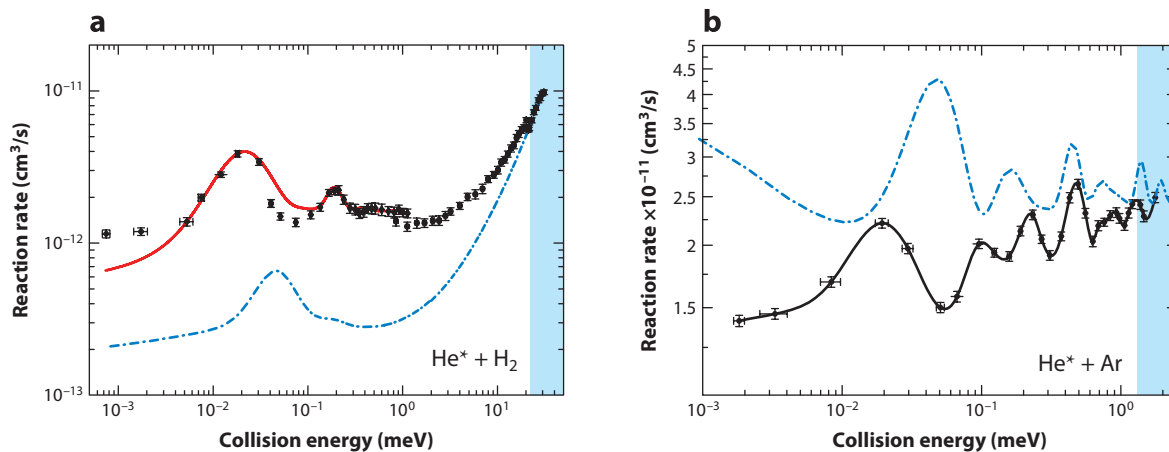
Figure 5

Penning ionization rates of metastable He* in ultracold collisions with (*a*) H_2 and (*b*) Ar atoms. The blue dashed-dotted lines are calculations using the best currently available potentials (119, 120). The solid red line in panel *a* is the calculated reaction rate using a modified Tang-Toennies potential with parameters chosen to best reproduce the experimental points; the solid black line in panel *b* is a guide to the eye. Shaded areas denote the lowest energy ranges achieved in previous measurements. Error bars are ±1 standard deviation. Figure reproduced from Reference 121, reprinted with permission from AAAS and E. Narevicius.

4. THEORETICAL PROGRESS

The rapid growth of experimental capabilities for cold atom-molecule and molecule-molecule collisions has been accompanied by equally prolific growth in theoretical techniques capable of treating the interaction as a truly quantum scattering problem (91, 122). At low and ultralow temperatures, the number of partial waves involved is sufficiently small that one must abandon the semiclassical approximation made by standard molecular dynamics and transition-state theories. However, the fully quantum problem is much harder computationally than the semiclassical one, so a great deal of research has been needed to find computationally tractable approximations.

Since the development of hyperfine coupled-channel methods by Alexander & Dagdigian (123) in the mid-1980s, improvements in both processing power and numerical methods have enabled sophisticated theoretical studies of molecule-atom and molecule-molecule collisions. Some recent examples include the work of Tscherbul et al. (124) considering YbF-He as a prototype for heavy-molecule-atom collisions, in which the nuclear hyperfine structure dominates over spin-rotation couplings, and the study undertaken by Gonzáles-Martínez & Hutson (125) of light NH-Mg collisions in a magnetic field. Tscherbul and Kłos performed a tour de force calculation of OH-ND_3 scattering in conjunction with the experimental results of Sawyer et al. (80) discussed above. Janssen et al. studied the full double-open-shell molecular problem in calculations of NH-NH elastic, inelastic (126), and reactive (127) scattering, and Quéméner and Bohn performed a set of coupled-channel calculations on OH-OH scattering (88, 104) motivated by our group's recent experimental results (88, 112). Cui & Krems (128) performed a more generic study of Zeeman relaxation and elastic collision rates in $^2\Sigma$ molecules.

A separate strand of development relies on multichannel quantum-defect theory (MQDT) methods (129). MQDT extends the normal coupled-channel formulation by formally uncoupling the input channels at some relatively small interparticle spacing, rather than integrating the Schrödinger equation from zero radius all the way to the maximum distance of interest. The method offers a reduction in algorithmic complexity from $O(N^3)$ to $O(N)$ (where N is the

number of channels) for studies involving the variation of parameters such as magnetic or electric fields, which is extremely attractive. MQDT has been applied to KRb losses (8), through both the recombination reaction given in Equation 1 and the reaction

$$KRb + K \rightarrow Rb + K_2 \tag{2}$$

with ultracold potassium atoms. It has also been used for general studies of molecular collisions in electric fields (130) and for an interesting demonstration of the transition from the ultracold regime of scattering theory to the more familiar regime of transition-state theory (131).

There have also been many recent efforts toward improved analytic treatments of diatomic molecules. Quéméner & Bohn (132) combined quantum threshold laws and a classical capture model to analytically derive the observed (dipole moment)[6] scaling of the KRb recombination rate. Idziaszek et al. (130) unified the MQDT and quantum threshold formalisms into a single model. Bohn & Quéméner (133) developed an analytic treatment of Hund's case A molecules subjected to crossed electric and magnetic fields, which they call case X and will substantially ease the design of future molecular trapping experiments. Bhattacharya et al. (134) recognized that the symmetry of the OH fine-structure ground state allows an analytic solution of the combined-field problem, which also includes the Λ-doublet.

Moreover, simple improvements in computational hardware speed mean that ab initio calculations of potential surfaces using density-functional theory followed by scattering calculations using those surfaces are now plausibly tractable for atom-molecule and even closed-shell diatom-diatom collisions. Virtually all the inelastic scattering results described in previous sections have been accompanied, or shortly followed, by ab initio calculations.

5. OUTLOOK

With such rapid improvements continuing in both experimental techniques and theoretical methods, there is no doubt that the future of cold molecules is bright. The development of laser cooled molecule sources (see the sidebar, Laser Cooling Molecules)—and especially molecular magneto-optical traps—will enable the entire toolkit of atomic physics to be brought to bear upon selected molecules. We note that of the results previously reviewed, almost all involve no molecules more massive, or higher-Z, than CO. This results in large part from the linear scaling of both the field strengths required to guide a molecule and the number of stages required to slow said molecule with the molecular mass-to-dipole moment ratio. Laser cooling techniques, however, sidestep this entirely. Indeed, two systems in which Doppler cooling has been demonstrated have mass over 100 amu, with one being a transition-metal oxide and the other an alkaline-earth fluoride; an optically pumped Sisyphus scheme has cooled CH_3F (135). The ability to bring these chemically diverse molecules to ultralow temperatures will enable completely new experiments.

Evaporative cooling is similarly an immensely powerful technique for reaching lower temperatures. On the pure physics side, the achievement of quantum degenerate dipolar gases is a long-standing goal, and evaporation is the most likely path to achieving that goal. Once the source molecules are cold enough to confine in an optical trap, they can be transferred to their absolute rotation-vibration-hyperfine ground state, at which point chemical recombination is the only collisional loss channel. It is now believed that many bialkali molecules (136), YO, and spin-polarized SrF (137) are stable against interchange reactions analogous to the reaction given in Equation 1. All these are therefore plausible candidates for creating molecular Bose-Einstein condensates or degenerate Fermi gases.

In summary, the outlook for ultracold molecular science is extremely exciting. Just as the field has come such a long way in the past five years, this review will likely seem substantially out of date in another five!

DISCLOSURE STATEMENT

The authors are not aware of any affiliations, memberships, funding, or financial holdings that might be perceived as affecting the objectivity of this review.

ACKNOWLEDGMENTS

LITERATURE CITED

1. Weiner J, Bagnato VS, Zilio S, Julienne PS. 1999. Experiments and theory in cold and ultracold collisions. *Rev. Mod. Phys.* 71:1–85
2. Chin C, Grimm R, Julienne P, Tiesinga E. 2010. Feshbach resonances in ultracold gases. *Rev. Mod. Phys.* 82:1225–86
3. Krems RV. 2005. Molecules near absolute zero and external field control of atomic and molecular dynamics. *Int. Rev. Phys. Chem.* 24:99–118
4. Doyle JM, Friedrich B, Krems RV, Masnou-Seeuws F. 2004. Quo vadis, cold molecules? *Eur. Phys. J. D* 31:149–64
5. Krems RV. 2008. Cold controlled chemistry. *Phys. Chem. Chem. Phys.* 10:4079–92
6. Ospelkaus S, Ni KK, Wang D, de Miranda MHG, Neyenhuis B, et al. 2010. Quantum-state controlled chemical reactions of ultracold potassium-rubidium molecules. *Science* 327:853–57
7. Bohn JL, Cavagnero M, Ticknor C. 2009. Quasi-universal dipolar scattering in cold and ultracold gases. *New J. Phys.* 11:055039
8. Idziaszek Z, Julienne PS. 2010. Universal rate constants for reactive collisions of ultracold molecules. *Phys. Rev. Lett.* 104:113202
9. Quéméner G, Bohn JL, Petrov A, Kotochigova S. 2011. Universalities in ultracold reactions of alkali-metal polar molecules. *Phys. Rev. A* 84:062703
10. Ticknor C. 2008. Collisional control of ground state polar molecules and universal dipolar scattering. *Phys. Rev. Lett.* 100:133202
11. Smith IWM, ed. 2008. *Low Temperatures and Cold Molecules*. London: Imperial Coll. Press
12. Krems RV, Stwalley WC, Friedrich B, eds. 2009. *Cold Molecules: Theory, Experiment, Applications*. Boca Raton, FL: CRC
13. **Carr LD, DeMille D, Krems RV, Ye J. 2009. Cold and ultracold molecules: science, technology and applications.** *New J. Phys.* **11:055049**
14. Friedrich B, Doyle JM. 2009. Why are cold molecules so hot? *ChemPhysChem* 10:604–23
15. Lemeshko M, Krems RV, Doyle JM, Kais S. 2013. Manipulation of molecules with electromagnetic fields. *Mol. Phys.* 111:1648–82
16. Bell MT, Softley TP. 2009. Ultracold molecules and ultracold chemistry. *Mol. Phys.* 107:99–132
17. Mestdagh J, Gaveau M, Gee C, Sublemontier O, Visticot J. 1997. Cluster isolated chemical reactions. *Int. Rev. Phys. Chem.* 16:215–47
18. Castleman AW, Keesee RG. 1986. Clusters: properties and formation. *Annu. Rev. Phys. Chem.* 37:525–50
19. Castleman AW, Wei S. 1994. Cluster reactions. *Annu. Rev. Phys. Chem.* 45:685–719
20. Toennies JP, Vilesov AF. 1998. Spectroscopy of atoms and molecules in liquid helium. *Annu. Rev. Phys. Chem.* 49:1–41
21. Callegari C, Lehmann KK, Schmied R, Scoles G. 2001. Helium nanodroplet isolation rovibrational spectroscopy: methods and recent results. *J. Chem. Phys.* 115:10090–110
22. Choi MY, Douberly GE, Falconer TM, Lewis WK, Lindsay CM, et al. 2006. Infrared spectroscopy of helium nanodroplets: novel methods for physics and chemistry. *Int. Rev. Phys. Chem.* 25:15–75

13. Provides a good introduction to cold molecules from a physicist's perspective.

23. Toennies JP. 2007. Molecular low energy collisions: past, present and future. *Phys. Scr.* 76:C15–20

24. Even U, Jortner J, Noy D, Lavie N, Cossart-Magos C. 2000. Cooling of large molecules below 1 K and He clusters formation. *J. Chem. Phys.* 112:8068–71

25. Hillenkamp M, Keinan S, Even U. 2003. Condensation limited cooling in supersonic expansions. *J. Chem. Phys.* 118:8699–705

26. Pentlehner D, Riechers R, Dick B, Slenczka A, Even U, et al. 2009. Rapidly pulsed helium droplet source. *Rev. Sci. Instrum.* 80:043302

27. Chefdeville S, Stoecklin T, Bergeat A, Hickson KM, Naulin C, Costes M. 2012. Appearance of low energy resonances in CO–*para*-H_2 inelastic collisions. *Phys. Rev. Lett.* 109:023201

28. Scoles G, ed. 1988. *Atomic and Molecular Beam Methods*. New York: Oxford Univ. Press

29. Rowe BR, Dupeyrat G, Marquette JB, Smith D, Adams NG, Ferguson EE. 1984. The reaction $O_2^+ + CH_4 \rightarrow CH_3O_2^+ + H$ studied from 20 to 560 K in a supersonic jet and in a SIFT. *J. Chem. Phys.* 80:241–45

30. Rowe BR, Dupeyrat G, Marquette JB, Gaucherel P. 1984. Study of the reactions $N_2^+ + 2N_2 \rightarrow N_4^+ + N_2$ and $O_2^+ + 2O_2 \rightarrow O_4^+ + O_2$ from 20 to 160 K by the CRESU technique. *J. Chem. Phys.* 80:4915–21

31. Smith IWM. 2006. Reactions at very low temperatures: gas kinetics at a new frontier. *Angew. Chem. Int. Ed. Engl.* 45:2842–61

32. Daranlot J, Jorfi M, Xie C, Bergeat A, Costes M, et al. 2011. Revealing atom-radical reactivity at low temperature through the N + OH reaction. *Science* 334:1538–41

33. Rellergert WG, Sullivan ST, Schowalter SJ, Kotochigova S, Chen K, Hudson ER. 2013. Evidence for sympathetic vibrational cooling of translationally cold molecules. *Nature* 495:490–94

34. Bell MT, Gingell AD, Oldham JM, Softley TP, Willitsch S. 2009. Ion-molecule chemistry at very low temperatures: cold chemical reactions between Coulomb-crystallized ions and velocity-selected neutral molecules. *Faraday Discuss.* 142:73–91

35. Okada K, Suganuma T, Furukawa T, Takayanagi T, Wada M, Schuessler HA. 2013. Cold ion–polar-molecule reactions studied with a combined Stark-velocity-filter–ion-trap apparatus. *Phys. Rev. A* 87:043427

36. Elioff MS, Valentini JJ, Chandler DW. 2003. Subkelvin cooling NO molecules via "billiard-like" collisions with argon. *Science* 302:1940–43

37. Strecker KE, Chandler DW. 2008. Kinematic production of isolated millikelvin molecules. *Phys. Rev. A* 78:063406

38. Kay JJ, van de Meerakker SYT, Strecker KE, Chandler DW. 2009. Production of cold ND_3 by kinematic cooling. *Faraday Discuss.* 142:143–53

39. Patterson D, Schnell M, Doyle JM. 2013. Enantiomer-specific detection of chiral molecules via microwave spectroscopy. *Nature* 497:475–77

40. Ospelkaus S, Pe'er A, Ni KK, Zirbel JJ, Neyenhuis B, et al. 2008. Efficient state transfer in an ultracold dense gas of heteronuclear molecules. *Nat. Phys.* 4:622–26

41. Ni KK, Ospelkaus S, de Miranda MHG, Pe'er A, Neyenhuis B, et al. 2008. A high phase-space-density gas of polar molecules. *Science* 322:231–35

42. Chotia A, Neyenhuis B, Moses SA, Yan B, Covey JP, et al. 2012. Long-lived dipolar molecules and Feshbach molecules in a 3D optical lattice. *Phys. Rev. Lett.* 108:080405

43. Deiglmayr J, Grochola A, Repp M, Dulieu O, Wester R, Weidemüller M. 2010. Permanent dipole moment of LiCs in the ground state. *Phys. Rev. A* 82:032503

44. Repp M, Pires R, Ulmanis J, Heck R, Kuhnle ED, et al. 2013. Observation of interspecies ^{6}Li-^{133}Cs Feshbach resonances. *Phys. Rev. A* 87:010701

45. Tung SK, Parker C, Johansen J, Chin C, Wang Y, Julienne PS. 2013. Ultracold mixtures of atomic ^{6}Li and ^{133}Cs with tunable interactions. *Phys. Rev. A* 87:010702

46. Debatin M, Takekoshi T, Rameshan R, Reichsollner L, Ferlaino F, et al. 2011. Molecular spectroscopy for ground-state transfer of ultracold RbCs molecules. *Phys. Chem. Chem. Phys.* 13:18926–35

47. Żuchowski PS, Aldegunde J, Hutson JM. 2010. Ultracold RbSr molecules can be formed by magnetoassociation. *Phys. Rev. Lett.* 105:153201

48. Guérout R, Aymar M, Dulieu O. 2010. Ground state of the polar alkali-metal-atom–strontium molecules: potential energy curve and permanent dipole moment. *Phys. Rev. A* 82:042508

49. Hara H, Takasu Y, Yamaoka Y, Doyle JM, Takahashi Y. 2011. Quantum degenerate mixtures of alkali and alkaline-earth-like atoms. *Phys. Rev. Lett.* 106:205304

50. Brue DA, Hutson JM. 2012. Magnetically tunable Feshbach resonances in ultracold Li-Yb mixtures. *Phys. Rev. Lett.* 108:043201

51. Munchow F, Bruni C, Madalinski M, Gorlitz A. 2011. Two-photon photoassociation spectroscopy of heteronuclear YbRb. *Phys. Chem. Chem. Phys.* 13:18734–37

52. Ye J, Kimble HJ, Katori H. 2008. Quantum state engineering and precision metrology using state-insensitive light traps. *Science* 320:1734–38

53. Patterson D, Doyle JM. 2007. Bright, guided molecular beam with hydrodynamic enhancement. *J. Chem. Phys.* 126:154307

54. Willitsch S, Bell MT, Gingell AD, Procter SR, Softley TP. 2008. Cold reactive collisions between laser-cooled ions and velocity-selected neutral molecules. *Phys. Rev. Lett.* 100:043203

55. Motsch M, van Buuren LD, Sommer C, Zeppenfeld M, Rempe G, Pinkse PWH. 2009. Cold guided beams of water isotopologs. *Phys. Rev. A* 79:013405

56. Rangwala SA, Junglen T, Rieger T, Pinkse PWH, Rempe G. 2003. Continuous source of translationally cold dipolar molecules. *Phys. Rev. A* 67:043406

57. Rieger T, Junglen T, Rangwala SA, Rempe G, Pinkse PWH, Bulthuis J. 2006. Water vapor at a translational temperature of 1 K. *Phys. Rev. A* 73:061402

58. Sommer C, Motsch M, Chervenkov S, van Buuren LD, Zeppenfeld M, et al. 2010. Velocity-selected molecular pulses produced by an electric guide. *Phys. Rev. A* 82:013410

59. Bethlem HL, Berden G, Meijer G. 1999. Decelerating neutral dipolar molecules. *Phys. Rev. Lett.* 83:1558–61

60. Bochinski JR, Hudson ER, Lewandowski HJ, Meijer G, Ye J. 2003. Phase space manipulation of cold free radical OH molecules. *Phys. Rev. Lett.* 91:243001

61. van de Meerakker SYT, Vanhaecke N, Meijer G. 2006. Stark deceleration and trapping of OH radicals. *Annu. Rev. Phys. Chem.* 57:159–90

62. van de Meerakker SYT, Bethlem HL, Vanhaecke N, Meijer G. 2012. Manipulation and control of molecular beams. *Chem. Rev.* 112:4828–78

63. Hogan SD, Sprecher D, Andrist M, Vanhaecke N, Merkt F. 2007. Zeeman deceleration of H and D. *Phys. Rev. A* 76:023412

64. Hogan SD, Wiederkehr AW, Schmutz H, Merkt F. 2008. Magnetic trapping of hydrogen after multistage Zeeman deceleration. *Phys. Rev. Lett.* 101:143001

65. Narevicius E, Libson A, Parthey CG, Chavez I, Narevicius J, et al. 2008. Stopping supersonic oxygen with a series of pulsed electromagnetic coils: a molecular coilgun. *Phys. Rev. A* 77:051401

66. Narevicius E, Raizen MG. 2012. Toward cold chemistry with magnetically decelerated supersonic beams. *Chem. Rev.* 112:4879–89

67. van de Meerakker S, Vanhaecke N, van der Loo M, Groenenboom G, Meijer G. 2005. Direct measurement of the radiative lifetime of vibrationally excited OH radicals. *Phys. Rev. Lett.* 95:013003

68. Campbell WC, Groenenboom GC, Lu HI, Tsikata E, Doyle JM. 2008. Time-domain measurement of spontaneous vibrational decay of magnetically trapped NH. *Phys. Rev. Lett.* 100:083003

69. van de Meerakker SYT, Smeets PHM, Vanhaecke N, Jongma RT, Meijer G. 2005. Deceleration and electrostatic trapping of OH radicals. *Phys. Rev. Lett.* 94:023004

70. Sawyer BC, Lev BL, Hudson ER, Stuhl BK, Lara M, et al. 2007. Magnetoelectrostatic trapping of ground state OH molecules. *Phys. Rev. Lett.* 98:253002

71. Kleinert J, Haimberger C, Zabawa PJ, Bigelow NP. 2007. Trapping of ultracold polar molecules with a thin-wire electrostatic trap. *Phys. Rev. Lett.* 99:143002

72. Sawyer BC, Stuhl BK, Wang D, Yeo M, Ye J. 2008. Molecular beam collisions with a magnetically trapped target. *Phys. Rev. Lett.* 101:203203

73. van de Meerakker SYT, Bethlem HL, Meijer G. 2008. Taming molecular beams. *Nat. Phys.* 4:595–602

74. **Hogan SD, Motsch M, Merkt F. 2011. Deceleration of supersonic beams using inhomogeneous electric and magnetic fields. *Phys. Chem. Chem. Phys.* 13:18705–23**

74. Comprehensively reviews Stark and Zeeman deceleration.

75. Meek SA, Parsons MF, Heyne G, Platschkowski V, Haak H, et al. 2011. A traveling wave decelerator for neutral polar molecules. *Rev. Sci. Instrum.* 82:093108

76. Quintero-Pérez M, Jansen P, Wall TE, van den Berg JE, Hoekstra S, Bethlem HL. 2013. Static trapping of polar molecules in a traveling wave decelerator. *Phys. Rev. Lett.* 110:133003

77. Egorov D, Lahaye T, Schöllkopf W, Friedrich B, Doyle JM. 2002. Buffer-gas cooling of atomic and molecular beams. *Phys. Rev. A* 66:043401

78. Hutzler NR, Lu HI, Doyle JM. 2012. The buffer gas beam: an intense, cold, and slow source for atoms and molecules. *Chem. Rev.* 112:4803–27

79. Patterson D, Rasmussen J, Doyle JM. 2009. Intense atomic and molecular beams via neon buffer-gas cooling. *New J. Phys.* 11:055018

80. Sawyer BC, Stuhl BK, Yeo M, Tscherbul TV, Hummon MT, et al. 2011. Cold heteromolecular dipolar collisions. *Phys. Chem. Chem. Phys.* 13:19059–66

81. Weinstein JD, deCarvalho R, Guillet T, Friedrich B, Doyle JM. 1998. Magnetic trapping of calcium monohydride molecules at millikelvin temperatures. *Nature* 395:148–50

82. deCarvalho R, Doyle JM, Friedrich B, Guillet T, Kim J, et al. 1999. Buffer-gas loaded magnetic traps for atoms and molecules: a primer. *Eur. Phys. J. D* 7:289–309

83. Lu HI, Rasmussen J, Wright MJ, Patterson D, Doyle JM. 2011. A cold and slow molecular beam. *Phys. Chem. Chem. Phys.* 13:18986–90

84. van Buuren LD, Sommer C, Motsch M, Pohle S, Schenk M, et al. 2009. Electrostatic extraction of cold molecules from a cryogenic reservoir. *Phys. Rev. Lett.* 102:033001

85. Sommer C, van Buuren LD, Motsch M, Pohle S, Bayerl J, et al. 2009. Continuous guided beams of slow and internally cold polar molecules. *Faraday Discuss.* 142:203–20

86. Campbell WC, Tsikata E, Lu HI, van Buuren LD, Doyle JM. 2007. Magnetic trapping and Zeeman relaxation of NH ($X^3\Sigma_-$). *Phys. Rev. Lett.* 98:213001

87. Tsikata E, Campbell WC, Hummon MT, Lu HI, Doyle JM. 2010. Magnetic trapping of NH molecules with 20 s lifetimes. *New J. Phys.* 12:065028

88. Stuhl BK, Hummon MT, Yeo M, Quéméner G, Bohn JL, Ye J. 2012. Evaporative cooling of the dipolar hydroxyl radical. *Nature* 492:396–400

89. Cornell EA, Wieman CE. 2002. Nobel lecture: Bose-Einstein condensation in a dilute gas, the first 70 years and some recent experiments. *Rev. Mod. Phys.* 74:875–93

90. Ketterle W, van Druten N. 1996. Evaporative cooling of trapped atoms. *Adv. At. Mol. Opt. Phys.* 37:181–236

91. Quéméner G, Julienne PS. 2012. Ultracold molecules under control! *Chem. Rev.* 112:4949–5011

92. Lara M, Bohn JL, Potter DE, Soldan P, Hutson JM. 2006. Ultracold Rb-OH collisions and prospects for sympathetic cooling. *Phys. Rev. Lett.* 97:183201

93. Żuchowski PS, Hutson JM. 2009. Low-energy collisions of NH_3 and ND_3 with ultracold Rb atoms. *Phys. Rev. A* 79:062708

94. Campbell W, Tscherbul T, Lu H, Tsikata E, Krems R, Doyle J. 2009. Mechanism of collisional spin relaxation in $^3\Sigma$ molecules. *Phys. Rev. Lett.* 102:013003

95. Ni KK, Ospelkaus S, Wang D, Quéméner G, Neyenhuis B, et al. 2010. Dipolar collisions of polar molecules in the quantum regime. *Nature* 464:1324–28

96. Parazzoli LP, Fitch NJ, Żuchowski PS, Hutson JM, Lewandowski HJ. 2011. Large effects of electric fields on atom-molecule collisions at millikelvin temperatures. *Phys. Rev. Lett.* 106:193201

97. Ticknor C, Bohn JL. 2005. Influence of magnetic fields on cold collisions of polar molecules. *Phys. Rev. A* 71:022709

98. Quéméner G, Bohn JL. 2010. Electric field suppression of ultracold confined chemical reactions. *Phys. Rev. A* 81:060701

99. Janssen LMC, Żuchowski PS, van der Avoird A, Groenenboom GC, Hutson. 2011. Cold and ultracold NH-NH collisions in magnetic fields. *Phys. Rev. A* 83:022713

100. Suleimanov YV, Tscherbul TV, Krems RV. 2012. Efficient method for quantum calculations of molecule-molecule scattering properties in a magnetic field. *J. Chem. Phys.* 137:024103

101. Kay JJ, van de Meerakker SYT, Strecker KE, Chandler DW. 2009. Production of cold ND_3 by kinematic cooling. *Faraday Discuss.* 142:143–53

102. de Miranda MHG, Chotia A, Neyenhuis B, Wang D, Quéméner G, et al. 2011. Controlling the quantum stereodynamics of ultracold bimolecular reactions. *Nat. Phys.* 7:502–7

103. Stuhl BK, Yeo M, Sawyer BC, Hummon MT, Ye J. 2012. Microwave state transfer and adiabatic dynamics of magnetically trapped polar molecules. *Phys. Rev. A* 85:033427

104. Quéméner G, Bohn JL. 2013. Ultracold molecular collisions in combined electric and magnetic fields. *Phys. Rev. A* 88:012706

105. Fagnan DE, Wang J, Zhu C, Djuricanin P, Klappauf BG, et al. 2009. Observation of quantum diffractive collisions using shallow atomic traps. *Phys. Rev. A* 80:022712

106. Tscherbul TV, Pavlovic Z, Sadeghpour HR, Côté R, Dalgarno A. 2010. Collisions of trapped molecules with slow beams. *Phys. Rev. A* 82:022704

107. Maussang K, Egorov D, Helton JS, Nguyen SV, Doyle JM. 2005. Zeeman relaxation of CaF in low-temperature collisions with helium. *Phys. Rev. Lett.* 94:123002

108. Lu MJ, Weinstein JD. 2009. Cold TiO($X^3\Delta$)-He collisions. *New J. Phys.* 11:055015

109. Hummon MT, Tscherbul TV, Kłos J, Lu HI, Tsikata E, et al. 2011. Cold N + NH collisions in a magnetic trap. *Phys. Rev. Lett.* 106:053201

110. Singh V, Hardman KS, Tariq N, Lu MJ, Ellis A, et al. 2012. Chemical reactions of atomic lithium and molecular calcium monohydride at 1 K. *Phys. Rev. Lett.* 108:203201

111. Singh V, Hardman KS, Lu MJ, Ellis A, Morrison MJ, Weinstein JD. 2013. Inelastic collisions of CaH with He at cryogenic temperatures. *Mol. Phys.* 111:1711–15

112. Stuhl BK, Yeo M, Hummon MT, Ye J. 2013. Electric-field-induced inelastic collisions between magnetically trapped hydroxyl radicals. *Mol. Phys.* 111:1798–804

113. Gilijamse JJ, Hoekstra S, van de Meerakker SYT, Groenenboom GC, Meijer G. 2006. Near-threshold inelastic collisions using molecular beams with a tunable velocity. *Science* 313:1617–20

114. Kirste M, Scharfenberg L, Kłos J, Lique F, Alexander MH, et al. 2010. Low-energy inelastic collisions of OH radicals with He atoms and D_2 molecules. *Phys. Rev. A* 82:042717

115. Scharfenberg L, Kłos J, Dagdigian PJ, Alexander MH, Meijer G, van de Meerakker SYT. 2010. State-to-state inelastic scattering of Stark-decelerated OH radicals with Ar atoms. *Phys. Chem. Chem. Phys.* 12:10660–70

116. Scharfenberg L, Gubbels K, Kirste M, Groenenboom G, van der Avoird A, et al. 2011. Scattering of Stark-decelerated OH radicals with rare-gas atoms. *Eur. Phys. J. D* 65:189–98

117. Kirste M, Wang X, Schewe HC, Meijer G, van der Avoird A, et al. 2012. Quantum-state resolved bimolecular collisions of velocity-controlled OH with NO radicals. *Science* 338:1060–63

118. Vanhaecke N, Meier U, Andrist M, Meier BH, Merkt F. 2007. Multistage Zeeman deceleration of hydrogen atoms. *Phys. Rev. A* 75:031402

119. Martin DW, Weiser C, Sperlein RF, Bernfeld DL, Siska PE. 1989. Collision energy dependence of product branching in Penning ionization: He⋆(2^1S, 2^3S) + H_2, D_2, and HD. *J. Chem. Phys.* 90:1564–76

120. Burdenski S, Feltgen R, Lichterfeld F, Pauly H. 1981. Total and ionization cross sections for He⋆(2^3S)–Ar and He⋆(2^1S)–Ar in the thermal energy range. *Chem. Phys. Lett.* 78:296–300

121. Henson AB, Gersten S, Shagam Y, Narevicius J, Narevicius E. 2012. Observation of resonances in Penning ionization reactions at sub-Kelvin temperatures in merged beams. *Science* 338:234–38

122. Herschbach D. 2009. Molecular collisions, from warm to ultracold. *Faraday Discuss.* 142:9–23

123. Alexander MH, Dagdigian PJ. 1985. Collision-induced transitions between molecular hyperfine levels: quantum formalism, propensity rules, and experimental study of CaBr($X^2\Sigma^+$) + Ar. *J. Chem. Phys.* 83:2191–200

124. Tscherbul TV, Kłos J, Rajchel L, Krems RV. 2007. Fine and hyperfine interactions in cold YbF-He collisions in electromagnetic fields. *Phys. Rev. A* 75:033416

125. González-Martínez ML, Hutson JM. 2011. Effect of hyperfine interactions on ultracold molecular collisions: NH($^3\Sigma^-$) with Mg(^1S) in magnetic fields. *Phys. Rev. A* 84:052706

126. Janssen LMC, Żuchowski PS, van der Avoird A, Groenenboom GC, Hutson JM. 2011. Cold and ultracold NH-NH collisions in magnetic fields. *Phys. Rev. A* 83:022713

127. Janssen LMC, van der Avoird A, Groenenboom GC. 2013. Quantum reactive scattering of ultracold NH($X^3\Sigma^-$) radicals in a magnetic trap. *Phys. Rev. Lett.* 110:063201

128. Cui J, Krems RV. 2013. Elastic and inelastic collisions of $^2\Sigma$ molecules in a magnetic field. *Phys. Rev. A* 88:042705

129. Provides a full description of MQDT as applied to molecular collisions.

129. Croft JFE, Wallis AOG, Hutson JM, Julienne PS. 2011. Multichannel quantum defect theory for cold molecular collisions. *Phys. Rev. A* 84:042703

130. Idziaszek Z, Quéméner G, Bohn JL, Julienne PS. 2010. Simple quantum model of ultracold polar molecule collisions. *Phys. Rev. A* 82:020703

131. Gao B. 2010. Universal model for exoergic bimolecular reactions and inelastic processes. *Phys. Rev. Lett.* 105:263203

132. Quéméner G, Bohn JL. 2010. Strong dependence of ultracold chemical rates on electric dipole moments. *Phys. Rev. A* 81:022702

133. Bohn JL, Quéméner G. 2013. Dipolar radicals in crossed electric and magnetic fields. *Mol. Phys.* 111:1931–38

134. Bhattacharya M, Howard Z, Kleinert M. 2013. Ground-state OH molecule in combined electric and magnetic fields: analytic solution of the effective Hamiltonian. *Phys. Rev. A* 88:012503

135. Zeppenfeld M, Englert BGU, Glockner R, Prehn A, Mielenz M, et al. 2012. Sisyphus cooling of electrically trapped polyatomic molecules. *Nature* 491:570–73

136. Żuchowski PS, Hutson JM. 2010. Reactions of ultracold alkali-metal dimers. *Phys. Rev. A* 81:060703

137. Meyer ER, Bohn JL. 2011. Chemical pathways in ultracold reactions of SrF molecules. *Phys. Rev. A* 83:032714

138. Hänsch T, Schawlow A. 1975. Cooling of gases by laser radiation. *Opt. Commun.* 13:68–69

139. Phillips WD. 1998. Nobel lecture: laser cooling and trapping of neutral atoms. *Rev. Mod. Phys.* 70:721–41

140. Bahns JT, Stwalley WC, Gould PL. 1996. Laser cooling of molecules: a sequential scheme for rotation, translation, and vibration. *J. Chem. Phys.* 104:9689–97

141. Stuhl BK, Sawyer BC, Wang D, Ye J. 2008. Magneto-optical trap for polar molecules. *Phys. Rev. Lett.* 101:243002

142. Shuman ES, Barry JF, Glenn DR, DeMille D. 2009. Radiative force from optical cycling on a diatomic molecule. *Phys. Rev. Lett.* 103:223001

143. Shuman ES, Barry JF, DeMille D. 2010. Laser cooling of a diatomic molecule. *Nature* 467:820–23

144. Barry J, Shuman E, Norrgard E, DeMille D. 2012. Laser radiation pressure slowing of a molecular beam. *Phys. Rev. Lett.* 108:103002

145. Hummon MT, Yeo M, Stuhl BK, Collopy AL, Xia Y, Ye J. 2013. 2D magneto-optical trapping of diatomic molecules. *Phys. Rev. Lett.* 110:143001

146. Zhelyazkova V, Cournol A, Wall TE, Matsushima A, Hudson JJ, et al. 2013. *Laser cooling and slowing of CaF molecules*. Unpublished manuscript. arXiv:1308.0421

Contents

Indexes

Errata

An online log of corrections to *Annual Review of Physical Chemistry* articles may be
found at http://www.annualreviews.org/errata/physchem

ANNUAL REVIEWS
It's about time. Your time. It's time well spent.

New From Annual Reviews:

Annual Review of Statistics and Its Application

Volume 1 • Online January 2014 • http://statistics.annualreviews.org

Editor: **Stephen E. Fienberg,** *Carnegie Mellon University*

Associate Editors: **Nancy Reid,** *University of Toronto*

Stephen M. Stigler, *University of Chicago*

The *Annual Review of Statistics and Its Application* aims to inform statisticians and quantitative methodologists, as well as all scientists and users of statistics about major methodological advances and the computational tools that allow for their implementation. It will include developments in the field of statistics, including theoretical statistical underpinnings of new methodology, as well as developments in specific application domains such as biostatistics and bioinformatics, economics, machine learning, psychology, sociology, and aspects of the physical sciences.

Complimentary online access to the first volume will be available until January 2015.

TABLE OF CONTENTS:

Access this and all other Annual Reviews journals via your institution at www.annualreviews.org.